



Observation of the Decay $K^- \rightarrow \pi^- \mu^+ \mu^-$ and Measurements of the Branching Ratios for $K^\pm \rightarrow \pi^\pm \mu^+ \mu^-$

H.K. Park,⁸ R.A. Burnstein,⁵ A. Chakravorty,⁵ A. Chan,¹ Y.C. Chen,¹ W.S. Choong,^{2,7} K. Clark,⁹ E.C. Dukes,¹⁰ C. Durandet,¹⁰ J. Felix,⁴ G. Gidal,⁷ P. Gu,⁷ H.R. Gustafson,⁸ C. Ho,¹ T. Holmstrom,¹⁰ M. Huang,¹⁰ C. James,³ C.M. Jenkins,⁹ D.M. Kaplan,⁵ L.M. Lederman,⁵ N. Leros,⁶ M.J. Longo,⁸ F. Lopez,⁸ L. Lu,¹⁰ W. Luebke,⁵ K.B. Luk,² K.S. Nelson,¹⁰ J.P. Perroud,⁶ D. Rajaram,⁵ H.A. Rubin,⁵ P.K. Teng,¹ J. Volk,³ C. White,⁵ S. White,⁵ and P. Zyla⁷

(HyperCP Collaboration)

¹*Institute of Physics, Academia Sinica, Taipei 11529, Taiwan, Republic of China*

²*University of California, Berkeley, California 94720*

³*Fermi National Accelerator Laboratory, Batavia, Illinois 60510*

⁴*University of Guanajuato, 37000 Leon, Mexico*

⁵*Illinois Institute of Technology, Chicago, Illinois 60616*

⁶*University of Lausanne, CH-1015 Lausanne, Switzerland*

⁷*Lawrence Berkeley National Laboratory, Berkeley, California 94720*

⁸*University of Michigan, Ann Arbor, Michigan 48109*

⁹*University of South Alabama, Mobile, Alabama 36688*

¹⁰*University of Virginia, Charlottesville, Virginia 22904*

(Dated: October 8, 2001)

Using data collected with the HyperCP (E871) spectrometer during the 1997 fixed-target run at Fermilab, we report the first observation of the decay $K^- \rightarrow \pi^- \mu^+ \mu^-$ and new measurements of the branching ratios for $K^\pm \rightarrow \pi^\pm \mu^+ \mu^-$. By combining the branching ratios for the decays $K^+ \rightarrow \pi^+ \mu^+ \mu^-$ and $K^- \rightarrow \pi^- \mu^+ \mu^-$, we measure $\Gamma(K^\pm \rightarrow \pi^\pm \mu^+ \mu^-)/\Gamma(K^\pm \rightarrow \text{all}) = (9.8 \pm 1.0 \pm 0.5) \times 10^{-8}$. The CP asymmetry between the rates of the two decay modes is $[\Gamma(K^+ \rightarrow \pi^+ \mu^+ \mu^-) - \Gamma(K^- \rightarrow \pi^- \mu^+ \mu^-)]/[\Gamma(K^+ \rightarrow \pi^+ \mu^+ \mu^-) + \Gamma(K^- \rightarrow \pi^- \mu^+ \mu^-)] = -0.02 \pm 0.11 \pm 0.04$.

PACS numbers: 13.20.Eb, 14.40.Aq, 11.30.Er

The rare decay of charged K mesons to a pion and a lepton pair ($K_{\pi ll}^\pm$, where $l = e$ or μ) can be used to study flavor-changing neutral currents as a higher-order process in the standard model and to explore new physics. However, to realize these goals, it is necessary to understand the dominant $K^\pm \rightarrow \pi^\pm \gamma^*$ radiative transition which involves long-distance hadronic effects. Since it is difficult to calculate such effects, chiral perturbation theory (ChPT) including electroweak interactions has been applied to $K_{\pi ll}^+$ [1]. In a recent model-independent analysis with ChPT at $\mathcal{O}(p^6)$ [2], the $K_{\pi ll}^+$ decay rate and the form factor characterizing the dilepton invariant-mass spectrum are calculated in terms of two parameters a_+ and b_+ . Determining these parameters from the measured branching ratio and the dilepton mass spectrum of the $K_{\pi ee}^+$ decay, this analysis predicts the ratio $\mathcal{R} = B(K_{\pi\mu\mu}^+)/B(K_{\pi ee}^+)$ to be greater than 0.23 and an increase in the CP asymmetry between the decay rates of $K_{\pi ll}^+$ and $K_{\pi ll}^-$ compared to the leading-order estimation in the chiral expansion [3]. The resulting expected CP asymmetry is $\sim 10^{-5}$ [2, 3].

The $K_{\pi ee}^+$ decay has been studied by several experiments [4–6], and the Particle Data Group (PDG) has compiled a mean branching ratio $B(K_{\pi ee}^+) = (2.88 \pm 0.13) \times 10^{-7}$ [7]. The $K_{\pi\mu\mu}^+$ decay was first observed by the E787 Collaboration at the Brookhaven National Laboratory (BNL). With 13 fully reconstructed 3-track

and 196 partially reconstructed 2-track events, they determined $B(K_{\pi\mu\mu}^+) = [5.0 \pm 0.4(\text{stat}) \pm 0.7(\text{syst}) \pm 0.6(\text{theor})] \times 10^{-8}$ [8]. The E865 Collaboration at BNL has subsequently observed 430 fully reconstructed $K_{\pi\mu\mu}^+$ events and measured $B(K_{\pi\mu\mu}^+) = [9.22 \pm 0.60(\text{stat}) \pm 0.49(\text{syst})] \times 10^{-8}$ [9]. The discrepancy between these two experimental results is more than three standard deviations and is not understood. In addition the value of \mathcal{R} obtained with the E787 result and the average value of $B(K_{\pi ee}^+)$ is inconsistent with the prediction and is difficult to accommodate within the standard model [2]. It is thus important to resolve the discrepancy in the $B(K_{\pi\mu\mu}^+)$ measurements.

In this Letter we present results on the first observation of $K^- \rightarrow \pi^- \mu^+ \mu^-$ decay, the branching ratios of $K_{\pi\mu\mu}^\pm$ decays, and a limit on their CP asymmetry. The HyperCP (E871) experiment in the Meson Center beam line of Fermilab, which was designed primarily to study CP violation in Ξ^-/Ξ^+ and $\Lambda/\bar{\Lambda}$ decays, took data in 1997 and 1999. We report here on an analysis of the 1997 data. A plan view of the spectrometer is shown in Fig. 1; a detailed description is given elsewhere [10].

K^\pm 's were produced by directing an 800-GeV/ c proton beam, with a typical intensity of 1.2×10^{11} protons per 20-second spill, onto a 2-mm-square copper target. A target length of 22 (60) mm was used when taking positive (negative)-secondary-beam data. The secondary-

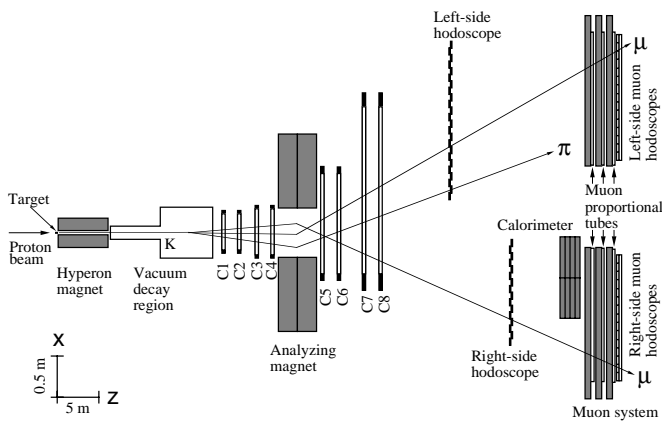


FIG. 1: Plan view of the HyperCP spectrometer. The length (width) of the spectrometer is about 62 m (4 m).

beam momentum was selected by a curved collimator embedded in a 6-m-long dipole magnet (Hyperon magnet) with a horizontal magnetic field of 1.67 T. The mean momentum of the secondaries was about 170 GeV/c, and the charge of the secondary beam was selected with the sign of the Hyperon magnet field. The typical secondary-beam rate was 13 MHz at the exit of the collimator. Following a 13-m evacuated decay pipe were eight multi-wire proportional chambers (C1–C8) with wire spacings increasing from 1 to 2 mm. A dipole magnet (Analyzing magnet) deflected charged particles horizontally with a transverse-momentum kick of 1.43 GeV/c. Particles with the same charge as the secondary beam were deflected to the left and those with opposite charge to the right. At the rear of the spectrometer were two scintillation hodoscopes and a calorimeter, used for triggering, and a muon detector system. The muon system consisted of two similar detectors on either side of the secondary beam line. The muon detectors had three layers of 0.81-m-thick steel absorber, each layer followed by a tracking station consisting of vertical and horizontal planes of proportional tubes with a pitch of 25.4 mm. At the rear of the third layer, behind the proportional tubes, were two orthogonal scintillator hodoscopes used for the muon triggers.

The $K_{\pi\mu\mu}^{\pm}$ rates were measured relative to the $K^{\pm} \rightarrow \pi^{\pm}\pi^{+}\pi^{-}$ ($K_{\pi 3}^{\pm}$) rates (the normalization mode). The trigger for the $K_{\pi 3}^{\pm}$ events was a heavily-prescaled coincidence of at least one hit in each of the left- and right-side hodoscopes. The trigger for the $K_{\pi\mu\mu}^{\pm}$ events, the unlike-sign dimuon trigger, required the presence of at least one hit in each hodoscope in the muon detectors in coincidence with hits in the left- and right-side hodoscopes. The sign of the secondary beam was changed every few hours by reversing the polarities of both the Hyperon and Analyzing magnets. The typical run cycle was two runs with positive secondary beam followed by one run with negative secondary beam.

Data for the $K_{\pi\mu\mu}^{\pm}$ and $K_{\pi 3}^{\pm}$ triggers were processed with the same reconstruction program. A three-track event topology was required. The sample of $K_{\pi\mu\mu}^{\pm}$ candidates was selected by requiring a muon track in each muon station and an unlike-sign dimuon trigger. The muon track was required to have hits in at least two of three muon chambers in both x and y views with corresponding in-time hits in the muon hodoscope. The algorithm for muon selection was checked using muon calibration data. The momentum of accepted muons was greater than 20 GeV/c.

Similar selection criteria were applied to both the signal ($K_{\pi\mu\mu}^{\pm}$) and normalization ($K_{\pi 3}^{\pm}$) event samples. One right-side track and two left-side tracks were required. Two pions from the $K_{\pi 3}^{\pm}$ decays were required to project to the same fiducial areas in the left- and right-side muon hodoscopes as the muons from the $K_{\pi\mu\mu}^{\pm}$ decays. The total momentum of the reconstructed tracks was required to lie between 120 and 250 GeV/c, consistent with the momentum spread of the secondary beam. To ensure that the kaons came from the target, the combined three-track momentum had to point back to within 5 mm of the center of the target in both x and y . The decay vertex of the three tracks was calculated by the method of distance of closest approach using the front track segments, and was required to be well within the vacuum decay region.

The $K_{\pi\mu\mu}^{\pm}$ and $K_{\pi 3}^{\pm}$ event candidates were required to have a decay topology consistent with a single vertex. This was done by first fitting the three tracks to a single vertex using the wire hits in C1–C4 and computing the χ^2 of the fit. In addition the average separation between the three pairs of tracks in the $x - y$ plane at the z position of the vertex determined by distance of closest approach was measured. Clean $K_{\pi 3}^{\pm}$ decays were used to study selection cuts based on the vertex-constrained-fit χ^2 and the average separation distance. Candidates were accepted if $\chi^2/ndf < 2.5$ and the average separation distance was less than 2 mm. These vertex cuts provided strong rejection of backgrounds, in particular those from two-vertex hyperon decays.

For events passing these cuts, the reconstructed three-track invariant mass $M_{\pi\mu\mu}$ distributions with a $K_{\pi\mu\mu}^{\pm}$ decay hypothesis are shown in Fig. 2. The signals in the vicinity of the kaon mass are clear and unambiguous.

To determine the branching ratios $B(K_{\pi\mu\mu}^{\pm}) = \Gamma(K^{\pm} \rightarrow \pi^{\pm}\mu^{+}\mu^{-})/\Gamma(K^{\pm} \rightarrow all)$ the following formula was used:

$$B(K_{\pi\mu\mu}^{\pm}) = \frac{N_{K_{\pi\mu\mu}^{\pm}}^{obs}}{200 \cdot N_{K_{\pi 3}^{\pm}}^{obs}} \frac{A_{K_{\pi 3}^{\pm}}}{A_{K_{\pi\mu\mu}^{\pm}}} \frac{\epsilon_{K_{\pi 3}^{\pm}}}{\epsilon_{K_{\pi\mu\mu}^{\pm}}} \frac{B(K_{\pi 3}^{\pm})}{\epsilon_{\mu^{+}\mu^{-}} \cdot \epsilon_{rel}^{trig}}, \quad (1)$$

where the N_i^{obs} 's are the numbers of observed events, the A_i 's are the geometrical acceptances, the ϵ_i 's are the event-selection efficiencies, ϵ_{rel}^{trig} is the relative trigger efficiency, and 200 is the prescale factor. The branching ratios $B(K_{\pi 3}^{\pm})$ are $(5.59 \pm 0.05)\%$ [7]. Unbinned

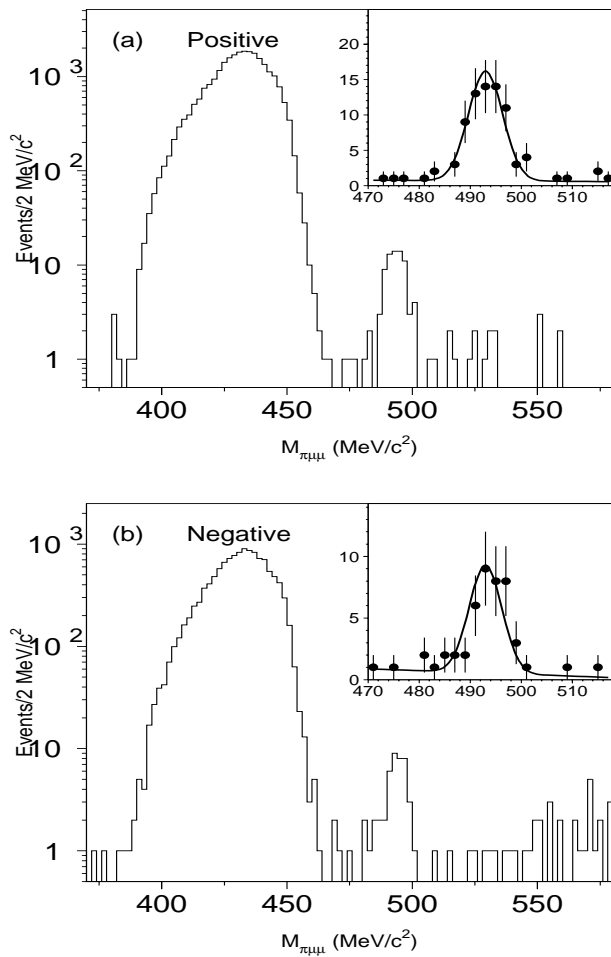


FIG. 2: The $\pi\mu\mu$ invariant mass distributions for (a) positive- and (b) negative-secondary-beam data after cuts. The large peak comes from $K_{\pi 3}^{\pm}$ events with in-flight decays of pions and pion punch-through to the muon stations. The inset shows the region around the kaon mass in more detail; points are data and the solid lines show the results of the likelihood fits.

maximum-likelihood fits for the events in the region $470 \text{ MeV}/c^2 < M_{\pi\mu\mu} < 520 \text{ MeV}/c^2$ were used to estimate the numbers of $K_{\pi\mu\mu}^{\pm}$ events, where the mass range for the fit was chosen to minimize the statistical error. Gaussian and linear functions were used to fit the signal and background respectively. The numbers of signal events from the fits were $N_{K_{\pi\mu\mu}^+}^{obs} = 65.3 \pm 8.2$ and $N_{K_{\pi\mu\mu}^-}^{obs} = 35.2 \pm 6.6$, where the errors are statistical. After background subtraction, the observed numbers of normalization events were $N_{K_{\pi 3}^+}^{obs} = (4.446 \pm 0.010) \times 10^5$ and $N_{K_{\pi 3}^-}^{obs} = (2.318 \pm 0.008) \times 10^5$, where the errors are dominated by the background estimation.

Background contributions to the $K_{\pi\mu\mu}^{\pm}$ samples from pion punch-through in the muon stations and in-flight decays of pions in $K_{\pi 3}^{\pm}$ decays and from $K^{\pm} \rightarrow \pi^+ \pi^- \mu^{\pm} \nu_{\mu}$ were negligible, mainly due to the good resolution of the spectrometer. Monte Carlo (MC) studies for these de-

cays showed that the reconstructed masses with the $\pi\mu\mu$ hypothesis of these modes were well below $480 \text{ MeV}/c^2$.

Many checks to verify the MC simulation were made. The kinematic parameters for K^{\pm} production at the target were tuned separately for the $K_{\pi 3}^+$ and $K_{\pi 3}^-$ normalization samples. The PDG Dalitz parameters for $K_{\pi 3}^{\pm}$ decays [7] were used in the MC program to properly simulate this decay. The distributions for kaon momenta and vertex positions of $K_{\pi 3}^{\pm}$ decays inside the decay pipe, hit positions of pions from the decays, and reconstructed masses were compared with data. They all showed good agreement.

In the simulation of $K_{\pi\mu\mu}^{\pm}$ decays, we assumed a vector interaction, based on the results of previous experiments [6, 9], and so the angular distribution of μ^+ in the rest frame of the virtual photon was generated according to the expression $(m_{\mu}^2 + p_{\mu}^2 \sin^2 \theta)$, where m_{μ} and p_{μ} are the mass and momentum of the muon, and θ is the angle between the directions of the μ^+ and the pion in this frame. In addition, we employed a form factor as described below. The dilepton invariant mass (M_{ll}) spectrum from the $K_{\pi ll}^{\pm}$ decays is described by the form factor $\phi(M_{ll}^2) = \phi_0(1 + \delta M_{ll}^2/m_{K^+}^2)$ where δ and ϕ_0 are a slope parameter and a constant, respectively, and m_{K^+} is the mass of the charged kaon [5, 6]. To extract δ , we averaged the measured values of the slope parameters determined by BNL E777 using $K_{\pi ee}^+$ decays [5] and by BNL E865 with $K_{\pi ee}^+$ [6] and $K_{\pi\mu\mu}^+$ events [9]. We obtained $\delta = 2.08 \pm 0.12$, where the error is only statistical. Figure 3 compares data for the dimuon invariant mass for $K_{\pi\mu\mu}^{\pm}$ decays with simulation results for 3 values of δ .

From the MC simulation the geometric acceptance for $K_{\pi 3}^{\pm}$ and $K_{\pi\mu\mu}^{\pm}$ decays inside the vacuum decay region for positive (negative)-secondary-beam data were estimated to be 94.4% (94.2%) and 47.5% (47.7%), respectively, where we have taken into account pion decay in flight and pion punch-through to the muon stations. Analyses identical to those applied to the data were used for the simulated normalization and signal events that passed the trigger requirements. The event selection efficiencies for $K_{\pi 3}^{\pm}$ and $K_{\pi\mu\mu}^{\pm}$ decays were 77.9% (76.0%) and 80.3% (78.3%) for positive (negative) secondary beam data respectively. The difference in efficiencies for K^+ and K^- events is primarily due to the slightly different momentum spectra for K^+ and K^- production. To estimate the trigger and dimuon selection efficiencies, the full data sample was used. Since the trigger for the normalization mode was common to that for the signal mode, we could determine the relative trigger efficiency for the signal mode with respect to the normalization mode. The relative trigger efficiency ϵ_{rel}^{trig} was found to be $(86.6 \pm 2.7)\%$. The dimuon selection efficiency $\epsilon_{\mu^+\mu^-}$ was $(93.8 \pm 0.3)\%$.

A summary of the systematic uncertainties is given in Table I. Systematic uncertainties on the measured branching ratios were minimized by using the same cuts both for the signal and for the normalization modes, with

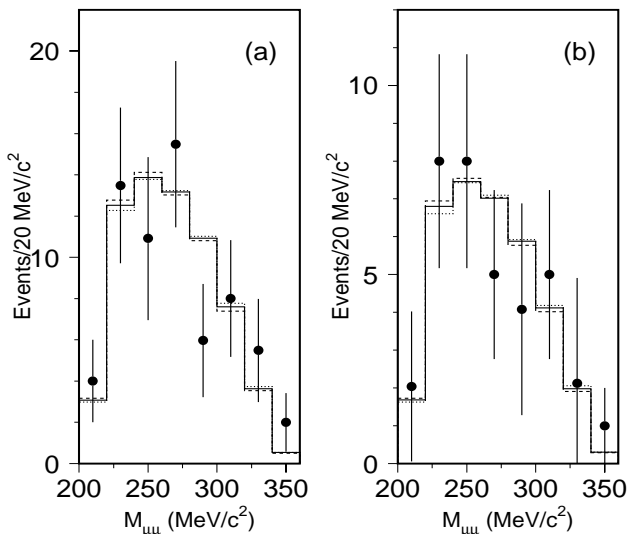


FIG. 3: The $\mu^+\mu^-$ invariant mass after background subtraction for (a) positive- and (b) negative-secondary-beam data after cuts. Points are data. The solid, dashed and dotted lines represent the simulation result with $\delta = 2.08, 1.72$ and 2.44 , respectively.

the exception of the muon-identification cuts which were applied to the signal events only. The major systematic uncertainties were the background estimation for the signal events and the trigger efficiency. In order to estimate the uncertainties in the numbers of signal events, various mass ranges were used for the fits, and fits with constant and quadratic functions for the background were used. The variations of the beam position at the target and the magnetic field strength in the Hyperon and Analyzing magnets during the run were monitored. By varying the assumed beam position, magnetic fields, K^\pm production parameters, and the decay parameters in the MC, we determined the sensitivity to these parameters of the relative acceptances and efficiencies for the signal and normalizing modes. Realistic ranges for these parameters were then used in computing the MC-dependent systematic uncertainties in Table I. Finally, the effect of the uncertainty in the slope parameter δ was estimated by varying it by three standard deviations (see Fig. 3), and found to be negligible.

Based on Eq. (1) we determined the branching ratios to be $B(K_{\pi\mu\mu}^+) = (9.7 \pm 1.2 \pm 0.4) \times 10^{-8}$ and $B(K_{\pi\mu\mu}^-) = (10.0 \pm 1.9 \pm 0.7) \times 10^{-8}$, where the first and second errors are statistical and systematic respectively. In terms of the partial decay rates $\Gamma(K_{\pi\mu\mu}^\pm)$, the CP asymmetry in these modes is defined as

$$\Delta(K_{\pi\mu\mu}^\pm) = \frac{\Gamma(K_{\pi\mu\mu}^+) - \Gamma(K_{\pi\mu\mu}^-)}{\Gamma(K_{\pi\mu\mu}^+) + \Gamma(K_{\pi\mu\mu}^-)}. \quad (2)$$

From our measurements of $B(K_{\pi\mu\mu}^\pm)$, we obtained

$$\Delta(K_{\pi\mu\mu}^\pm) = -0.02 \pm 0.11(\text{stat}) \pm 0.04(\text{syst}).$$

In conclusion, we have observed both $K^+ \rightarrow \pi^+\mu^+\mu^-$ and $K^- \rightarrow \pi^-\mu^+\mu^-$ decays and measured their branching ratios. This is the first observation of the $K^- \rightarrow \pi^-\mu^+\mu^-$ decay. The CP asymmetry parameter, $\Delta(K_{\pi\mu\mu}^\pm)$, has been extracted from these measurements. Our result is consistent with no CP violation. Assuming CP symmetry is valid, we can combine $B(K_{\pi\mu\mu}^+)$ and $B(K_{\pi\mu\mu}^-)$ to give a result of $[9.8 \pm 1.0(\text{stat}) \pm 0.5(\text{syst})] \times 10^{-8}$, which is 3.2 standard deviations higher than the BNL E787 measurement [8], but consistent with the BNL E865 result [9] and, using the PDG value for $B(K_{\pi ee}^+)$, is also consistent with the model-independent analysis for the \mathcal{R} value [2].

Source	σ_B/B (%)	$\sigma_B/B(K_{\pi\mu\mu}^\pm)$ (%)
Beam targeting	1.1 (0.9)	1.0
Magnetic field	0.5 (0.4)	0.5
Trigger efficiency	3.1 (3.1)	3.1
Muon identification	0.3 (0.3)	0.3
Background Estimation ($K_{\pi_3}^\pm$)	0.2 (0.3)	0.2
Background Estimation ($K_{\pi\mu\mu}^\pm$)	2.4 (6.4)	3.6
Data and MC disagreement	0.4 (0.4)	0.4
Dalitz parameter	0.3 (0.3)	0.3
Slope parameter (δ)	0.2 (0.3)	0.2
$B(K^+ \rightarrow \pi^+\pi^+\pi^-)$	0.9 (0.9)	0.9
Total	4.2 (7.3)	5.0

TABLE I: Summary of estimated systematic uncertainties in the branching ratios of $B(K_{\pi\mu\mu}^+)$, and, in parentheses, $B(K_{\pi\mu\mu}^-)$. The last column gives the systematic errors for the combined branching ratio, $B(K_{\pi\mu\mu}^\pm)$.

The authors are indebted to the staffs of Fermilab and the participating institutions for their vital contributions. This work was supported by the U.S. Department of Energy and the National Science Council of Taiwan, R.O.C.

-
- [1] G. Ecker, A. Pich and E. de Rafael, Nucl. Phys. B **291**, 692 (1987).
 - [2] G. D'Ambrosio, G. Ecker, G. Isidori and J. Portolés, JHEP **8**, 4 (1998).
 - [3] G. Ecker, A. Pich and E. de Rafael, Nucl. Phys. B **303**, 665 (1988).
 - [4] P. Bloch *et al.*, Phys. Lett. B **56**, 201 (1975).
 - [5] C. Alliegro *et al.*, Phys. Rev. Lett. **68**, 278 (1992).
 - [6] R. Appel *et al.*, Phys. Rev. Lett. **83**, 4482 (1999).
 - [7] Particle Data Group, D.E. Groom *et al.*, Eur. Phys. J. C **15**, 1 (2000).
 - [8] S. Adler *et al.*, Phys. Rev. Lett. **79**, 4756 (1997).
 - [9] H. Ma *et al.*, Phys. Rev. Lett. **84**, 2580 (2000).
 - [10] Y.C. Chen *et al.*, Nucl. Instrum. Methods A **455**, 424 (2000); W.S. Choong, Ph.D. thesis, University of California, Berkeley (2000).